Journal of Innovative Optical Health Sciences
Vol. 4, No. 3 (2011) 261–268

DOI: 10.1142/S1793545811001575

POWER OF DUAL-WAVELENGTH APPROACHES IN STUDYING PHYSIOLOGICAL AND FUNCTIONAL CHANGES OF INTACT HEART AND *IN VIVO* BRAIN*

ZHONGCHI LUO[†,¶] and CONGWU DU[‡,§,‖]
[†]*Department of Biomedical Engineering*
SUNY at Stony Brook, Stony Brook, NY 11794, USA
[‡]*Medical Department, Brookhaven National Laboratory*
Upton, NY 11973-5000, USA
[§]*Department of Anesthesiology, SUNY at Stony Brook*
Life Science Building, Room 002
Stony Brook, NY 11794, USA
[¶]*zluo@ic.sunysb.edu*
[‖]*congwu@bnl.gov*

Accepted 25 April 2011

Since the dual-wavelength spectrophotometer was developed, it has been widely used for studying biological samples and applied to extensive investigations of the electron transport in respiration and redox cofactors, redox state, metabolic control, and the generation of reactive oxygen species in mitochondria. Here, we discuss some extension of dual-wavelength approaches in our research to study the physiological and functional changes in intact hearts and *in vivo* brain. Specifically, we aimed at (1) making nonratiometric fluorescent indicator become ratiometric fluorescence function for investigation of Ca^{2+} dynamics in live tissue; (2) eliminating the effects of physiological changes on measurement of intracellular calcium; (3) permitting simultaneous imaging of multiple physiological parameters. The animal models of the perfused heart and transiently ischemic insult of brain are used to validate these approaches for physiological applications.

Keywords: Dual-wavelength; optical spectroscope and biomedical imaging; heart; brain; Rhod2 fluorescence.

1. Introduction

In 1950s, Britton Chance invented the dual-wavelength spectrophotometer,[1] which has been widely used for physiological studies, including bioenergetics, especially for trend measurements of hemoglobin oxygenation and of cytochrome oxidation.[2–8] To

*This manuscript is dedicated to the memory of Britton Chance who introduced me (C. Du) to NIR spectroscopy with dual-wavelength approach in 1996 at the University of Pennsylvania, USA.
‖Corresponding author.

compare with Millikan's dual-wavelength technique,[9] he improved the technology[10] to be very efficient for measuring small difference of absorption and rejecting changes of background light scattering since the two wavelengths that were selected by a pair of monochromators were quite close together.[1] Furthermore, this principle has been applied for near-infrared (NIR) measurement to characterize hemoglobin absorption; for example, while wavelength of 760 nm is responsive to the deoxy form, the wavelength of 850 nm is responsive to the oxy form, and the difference between the two was very nearly balanced in intensity by using filters of appropriate transmission bandwidth as demonstrated in his spectrophotometer.[10] Importantly, while the two wavelengths of λ_1 and λ_2 selected have absorbance symmetrical to that at isobestic wavelength (i.e. λ_{iso}) but with opposite direction (e.g., $\varepsilon_{Hbx}(\lambda_1) - \varepsilon_{Hbx}(\lambda_{iso}) \approx \varepsilon_{Hbx}(\lambda_{iso}) - \varepsilon_{Hbx}(\lambda_2)$, it can maximize the sensitivity of the optical measurement to the changes in the tissue oxygenation. In other words, the subtraction of the absorbance at λ_1 and λ_2 enhances oxy-deoxy changes of hemoglobin.[11] The sum of the absorbance can be used to give the total amount of hemoglobin.[10,11] This two-wavelength approach allows us to distinguish the hemoglobin oxygenation changes from the changes in total hemoglobin concentration (e.g., blood volume) in biological tissue such as brain. This technique has been validated for human studies, especially in measuring muscle and brain,[10–12] which now has been widely used for diagnosing diseases[10,13,14] (e.g., brain hypoxia, haematomas, etc.) and for functional activity study of brain (e.g., fNIRI).[3,15–17]

In our optical diffusion and fluorescence spectroscopy system, we adapt this dual-wavelength technology but within the visible region to determine the changes in the cerebral blood volume (CBV) and tissue oxygenation induced by ischemia[18] and stimulants (e.g., cocaine) in the rodent brain.[19] Here, we discuss more dual-wavelength approaches developed in our research, which focus on (1) making nonratiometric fluorescent indicator become ratiometric fluorescence function for investigation of Ca^{2+} dynamics in live tissue; (2) eliminating the effects of physiological changes on measurement of intracellular calcium; (3) permitting simultaneous imaging of multiple physiological parameters. The animal models of the perfused heart and transiently ischemic insult of brain are used to validate these approaches for physiological applications.

2. Dual-Wavelength Approach to Make Nonratiometric Fluorescence Indicator Become Ratiometric Function for $[Ca^{2+}]_i$ Measurement

The measurement of calcium (Ca^{2+}) transients is important to study a number of physiological characteristics of cardiac function. Fluorescence technology has demonstrated great potential for detection of Ca^{2+} transients in the perfused heart.[20–22] The noninvasive nature of the fluorescence method allows the beating heart to act at its own control, which is more physiological than isolated myocyte studies. However, the limitation of measuring Ca^{2+} transients in the whole heart model is the poor penetration of fluorescence excitation and emission because of the overwhelming scattering and strong absorption of tissue to ultraviolet (UV) light required for the traditional ratiometric Ca^{2+} indicators.

Ca^{2+} indicators excitable at the relatively longer wavelength, for example, with visible light region such as Rhod2, are commercially available. The advantages of these fluorescence dyes over the UV-excitable Ca^{2+} indicators are long excitation and emission wavelengths, which allows for greater penetration, and reduced interference from naturally occurring fluorescent compounds such as NAD(P)H. Moreover, the changes in fluorescence upon Ca^{2+} binding are high, e.g., a 100-fold increase in fluorescence when Rhod2 binds to Ca^{2+}. The disadvantage of Rhod2 is that there is no shift of either excitation or fluorescence emission spectra upon binding with Ca^{2+}, so that common ratiometric methods to quantify Ca^{2+} content cannot be used.[23]

Figure 1 shows the problem if we could not ratio, indicating the effects of Rhod2 washout on fluorescence emission. Figure 1(a) illustrates the loading of Ca^{2+} indicator into the intact heart. Specifically, Rhod2 (AM) (Invitrogen, 100 μg) is dissolved with dimethylsulfoxide (DMSO, 4 μL) and distilled water (200 μL), mixed with oxygenated Krebs solution (9 mL) and then is bolused through the perfusate. After 20–25 min, ~6-fold increase in fluorescence can be detected at 589 nm (λ_{em}) when excited at 524 nm (λ_{ex}). Ca^{2+}-dependent fluorescence transients along with the corresponding left ventricular pressure signals are acquired. Figure 1(b) shows the time course of the Ca^{2+}-dependent fluorescence signals of the transients (from diastole to systole, pink curves) and the mean fluorescence (black dots).

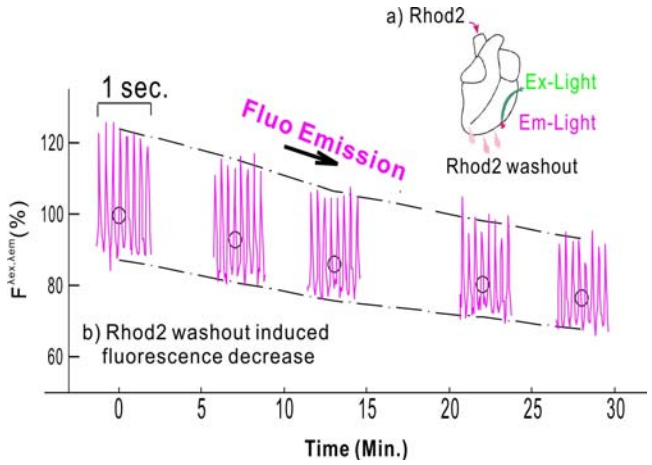

Fig. 1. (a) Rhod2 washout from the heart decreases; (b) fluorescence mean intensity (black hollow circles) and transients (magenta curves) as a function of time.

The attenuation of fluorescence emission as a function of time (both in the mean fluorescence and Ca^{2+} transient amplitude) is observed as shown in Fig. 1(b), thus indicating the effects of Rhod2 washout on fluorescence signals.

To overcome this problem, we come up with a strategy to measure the reflective absorbance at excitation wavelength of 524 nm (λ_{ex}) along with that at emission wavelength of 589 nm (λ_{em}). As the absorbance is Rhod2 sensitive at λ_{ex} but Rhod2 insensitive at λ_{em}, the ratio of the reflected absorbance at these two wavelengths (i.e. $A^{\lambda ex}/A^{\lambda em}$, hereafter abbreviated as $A^{\lambda ex,\lambda em}$) can be used as a measure of dye (i.e., Rhod2) concentration in tissue. Figure 2 shows the schematic of the absorbance measurements (by PMT-A) simultaneous with the Ca^{2+}-dependent fluorescence (by PMT-F) from the perfused heart. The ratio of the reflective absorbance between 524 nm and 589 nm (i.e., $A^{\lambda ex,\lambda em}$) is acquired from the heart by time-sharing using a flexible liquid light guide coupled to a photomultiplier tube PMT-A. The light guide is positioned at 45° on a vertical plane to avoid the specular reflection from the interfaces between the perfusion chamber and the heart surface.

Figure 3 shows the simultaneous measurement of Ca^{2+}-dependent fluorescence $F^{\lambda ex,\lambda em}$ and the absorbance $A^{\lambda ex,\lambda em}$ as a function of time. It is clearly

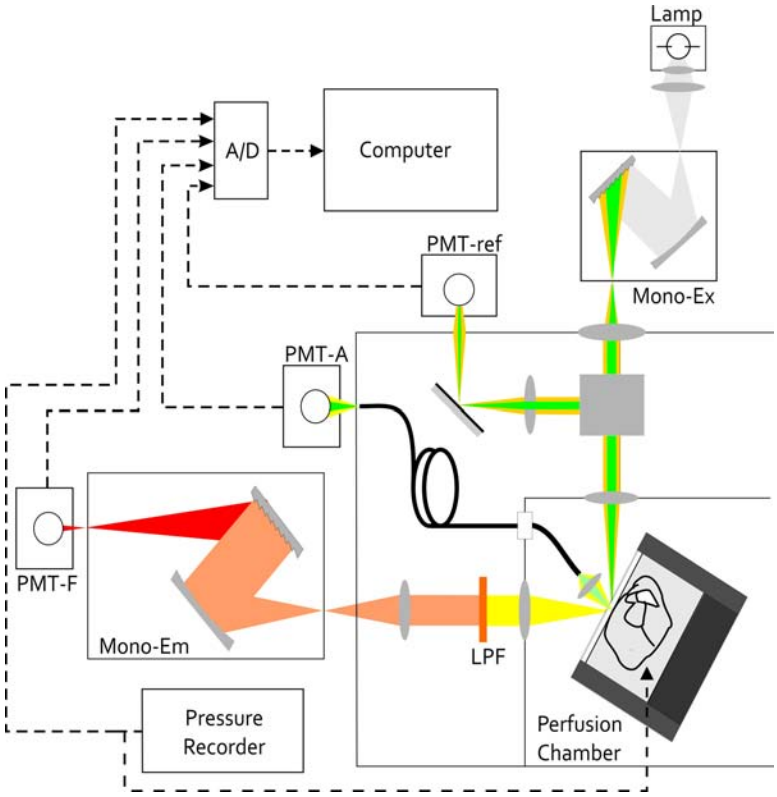

Fig. 2. A schematic of simultaneous fluorescence and absorbance measurements from the surface of intact heart under perfusion. Mono-Ex: monochromater for excitation wavelength; Mono-Em: monochromater for fluorescent emission wavelength; PMT-ref: reference photomultiplier tube for detecting light source fluctuation; PMT-A: PMT for detecting reflective absorbance; PMT-F: PMT for fluorescence detection; LPF: long pass filter to block excitation light.

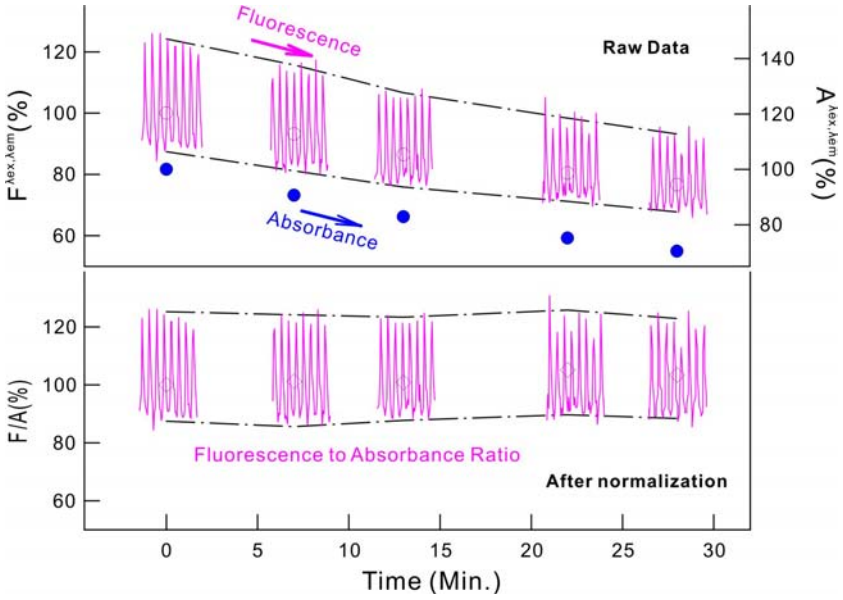

Fig. 3. Effects of Rhod2 washout from the heart on fluorescence mean intensity (black hollow circles) and transients (magenta curves) and absorbance (blue solid circles) (top panel) and the corrected measurement using fluorescence-to-absorbance ratio as a function of time (bottom panel).

shown that both fluorescence and absorbance signals decline at the same rate with time, which demonstrates a proportional impact of dye leakage on the fluorescence and absorbance measurements. More importantly, after normalizing by the absorbance, both the mean Ca^{2+} fluorescence and the transient amplitude remained unchanged with time, thus confirming that the ratiometric technique of $F^{\lambda ex,\lambda em}/A^{\lambda ex,\lambda em}$ can eliminate the effects of dye concentration changes on the $[Ca^{2+}]_i$ measurement for the physiological study of the heart.

3. Dual-Wavelength Approach to Minimize the Influence of Physiological Changes on Fluorescence Measurement

Although the excitation and emission of Rhod2 are in the visible range of 500−630 nm, where tissue chromophores (mainly myoglobin in perfused heart) absorb much less light than in the UV range, the tissue optical properties (absorption and scattering) still play an important role in the fluorescence detection. This so-called "inner filter" effect, to a great extent, depends on tissue oxygenation.[22] Figure 4 shows the reflective absorption spectra of myoglobin obtained from the surface of a perfused mouse heart with varying oxygenation state from normoxic (red dashed curve) to hypoxic (brown dashed curve). The corresponding fluorescence spectra of Rhod2 measured from the heart at these two states (i.e., normoxia and hypoxia) are superposed in Fig. 4 as well (i.e., pink and dark-red solid curves, respectively). It demonstrates that the fluorescence intensity of Rhod2 changes with the oxygenation of the heart, except at the isosbestic wavelengths (e.g., 589 nm etc). To minimize the influence of the tissue absorption changes caused by the oxygenation on the absorbance and fluorescence detection, two isosbestic wavelengths of $\lambda_{ex} = 524$ nm and $\lambda_{em} = 589$ nm with regards to myoglobin oxygenation are chosen for fluorescence excitation and emission detection. In addition, the reflectance spectra of heart tissue at 524 nm and 589 nm are approximately equivalent (i.e., $R^{\lambda ex} \sim R^{\lambda em}$ as illustrated in Fig. 4), thus implying a similar optical pathlength at these two wavelengths. Therefore, the influence of the potential fluctuation in tissue scattering on $F^{\lambda ex,\lambda em}$ or $A^{\lambda ex,\lambda em}$ can be minimized.

4. Dual-Wavelength Approach to Permit the Simultaneous Imaging for Multiphysiological Parameters

Compared with conventional nueroimaging modalities, e.g., fMRI and PET/SPECT, optical imaging techniques have the potential for high spatiotemporal resolutions and differentiation of the changes

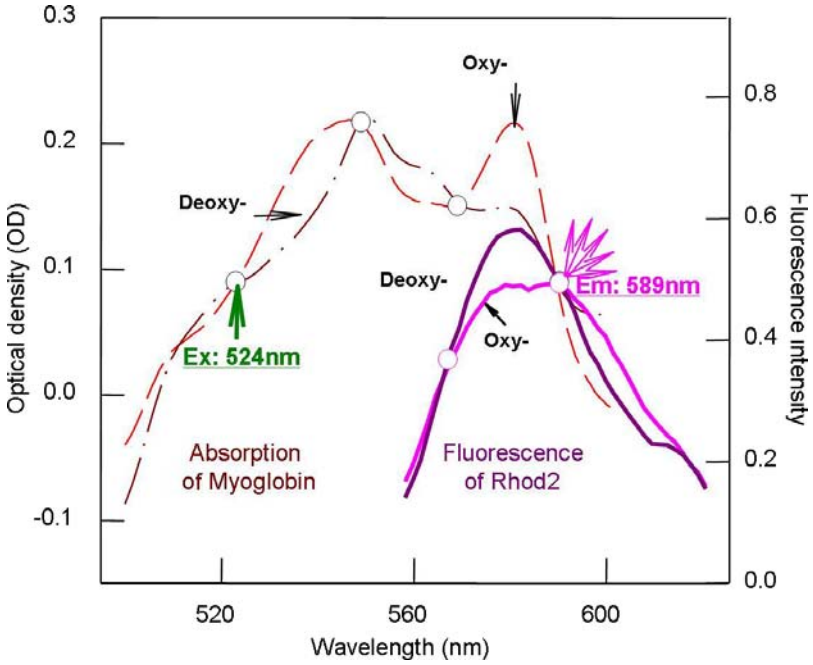

Fig. 4. Effects of oxygenation changes on myoglobin absorbance (dashed lines) in perfused heart and Rhod2 fluorescence spectra (solid lines), based on which two isosbestic points in the absorbance spectra at $\lambda_{ex} = 524$ and $\lambda_{em} = 589$ nm were selected as the excitation and detected emission wavelength for Ca^{2+}-dependent fluorescence measurement.

in cerebral blood flow (CBF), CBV and hemoglobin oxygenation and neuronal activities by utilizing a wide variety of optical effects, including Doppler effect, absorption, scattering, fluorescent labeling and photon-acoustic effects.[24,25] More importantly, simultaneous imaging of these parameters will immensely enhance our understanding of the processes that underlie neural activities and brain functions.

4.1. *Simultaneous imaging of hemodynamic and blood oxygenation changes in cortex*

Figure 5 illustrates our recently developed dual-wavelength ($\lambda_1 = 785$, $\lambda_2 = 830$ nm) laser speckle imaging technique (DW-LSCI) that enables concurrent imaging of changes in CBF, CBV (or total hemoglobin) and hemoglobin oxygenation (i.e., oxy-hemoglobin [HbO_2] and deoxy-hemoglobin [HbR]) at high spatiotemporal resolutions.[26] Figure 6 shows the results of the validating experiment using a transient ischemia model in rat forebrain. Figure 6(a) represents the CBF mapping of the rat cortical brain. Figures 6(b)–6(e) show the time courses of the changes of oxygenated-(b: Δ[HbO2]), deoxygenated-(c: Δ[HbR]) and total hemoglobin (d: [HbT]) along with blood flow changes (e, ΔCBF(%)) in large (blue) and small (red) vessels as well as the tissue area (green), illustrating the spatiotemporal hemodynamic and oxygenation changes induced by ischemia. The selected regions of interest (ROIs) are marked in Fig. 6(a). At the onset of reperfusion after 5-min ischemia, all the signals started to recover to their baselines in the perturbed cortical regions.

4.2. *Simultaneous imaging of CBF and $[Ca^{2+}]_i$ dynamics induced by ischemia and reperfusion*

To simultaneously image CBF changes along with the changes in intracellular calcium ($[Ca^{2+}]_i$) from the surface of the live brain, a green laser of 532 nm was added into our DW-LSCI system (Fig. 5). Rhod2 (12 μg) was slowly (~30 min) loaded into the brain cortex through a micropipette, and a ~60-min waiting period after the loading permits cellular uptake of Rhod2. The influence of the hemoglobin absorption on the fluorescence emission can be corrected empirically through CBF changes measured simultaneously.[27] Figure 7 shows the *in vivo* results of CBF (lower panel) and $[Ca^{2+}]_i$ fluorescence (upper panel) response to a transient ischemic insult, including the time lapsed mapping and the averaged time courses of $[Ca^{2+}]_i$ fluorescence

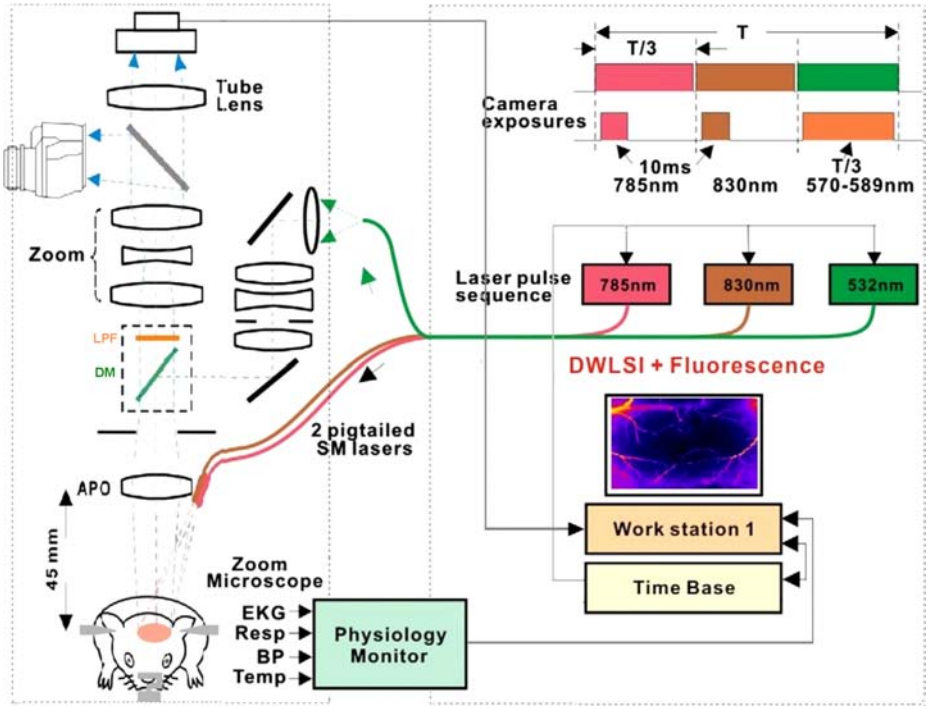

Fig. 5. Sketch illustrating the DW-LSCI setup. Laser diodes at 532 nm, 785 nm and 830 nm. LPF: longpass filter, DM: dichroic mirror, APO: Apochromatic objective.

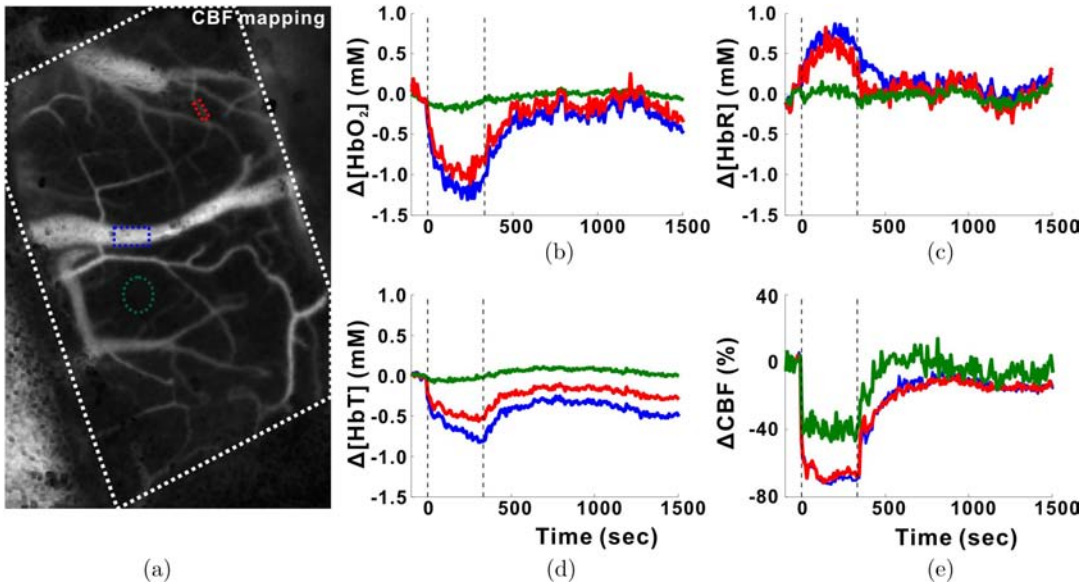

Fig. 6. (a) Snapshot of DW-LSCI cerebral blood flow (CBF) image of rat cortex and time course of (b) $\Delta[HbO_2]$, (c) $\Delta[HbR]$, (d) $\Delta[HbT]$ and (e) percentage CBF changes in the selected regions of interest (blue: a large vessel; red: a small vessel, green: selected tissue region) elicited by the ischemia and reperfusion challenge. The pair of dashed lines indicate the onset of ischemia ($t = 0$ min) and reperfusion ($t = 5$ min) periods.

[(a) 0−4 and (c)] and CBF [(b) 0−4 and (d)] change of the brain during the experiment. It shows the decrease in CBF and increase of $[Ca^{2+}]_i$ induced by ischemia, but both turned back towards recovery upon reperfusion. This demonstrates the capability of the two-wavelength approach for simultaneous imaging of CBF mapping and $[Ca^{2+}]_i$ fluorescence on a living brain.

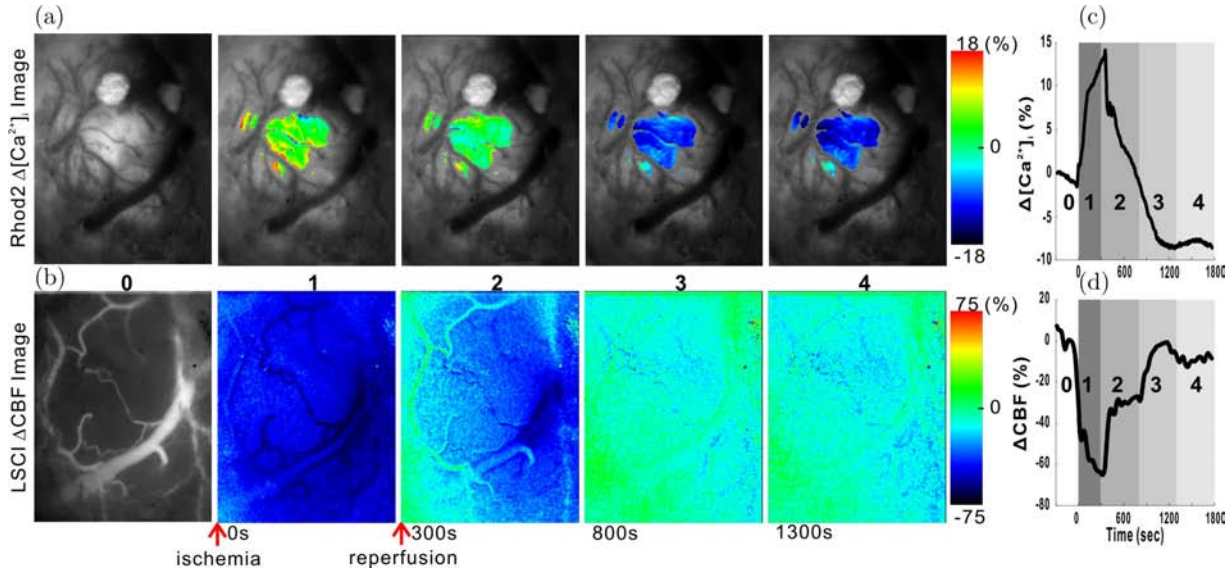

Fig. 7. The time-lapsed (a) Rhod2 fluorescent images of intracellular calcium changes and (b) LSCI CBF images during the ischemia-reperfusion insult (noted by the red arrow at the bottom of (d) as well as the darkest grey shadow on the time courses) and (e, f) their concurrent time courses averaged from the color mapped regions in (c) and (d) respectively.

5. Summary

In summary, we present the two-wavelength techniques developed in our laboratory which have been validated for the fluorescence measurement of $[Ca^{2+}]_i$ transients from the beating heart and for the optical neuroimaging of the *in vivo* brain. Specifically, we demonstrate that the fluorescence-to-absorbance ratio at two isosbestic wavelengths of 524 nm and 598 nm can be used to calibrate the changes of dye concentration due to wash-out during the heart perfusion as well as the changes of tissue oxygenation states. Adaptation of dual-wavelength to neuroimaging technique provides simultaneous imaging of multiple physiological parameters such as cerebral blood flow, hemoglobin oxygenation and intracellular calcium, thus distinguishing the cellular activation ($[Ca^{2+}]_i$) from vascular function (CBF) and tissue oxygen metabolism ($[HbO_2]$ and [HbR]). Our experimental results demonstrate the power of dual-wavelength techniques, which open new opportunities to study the function of normal or diseased organs (e.g., heart or brain) to understand their physiological and pathological processes for future medical intervention.

Acknowledgment

The experiments of heart perfusion were conducted in Carnegie Mellon University with Drs. Guy MacGowan and Alan Koretsky. The brain study is supported in part by NIH grants K25-DA021200, RC1-DA028534 and by Department of Energy grant LDRD 10-023 at Brookhaven National Laboratory.

References

1. B. Chance, "Rapid and sensitive spectrophotometry. III. A double beam apparatus," *Rev. Sci. Instrum.* **22**, 634–638 (1951).
2. B. Chance, J. S. Leigh, H. Miyake, D. S. Smith, S. Nioka, R. Greenfeld, M. Finander, K. Kaufmann, W. Levy, M. Young *et al.*, "Comparison of time-resolved and -unresolved measurements of deoxyhemoglobin in brain," *Proc. Natl. Acad. Sci. USA* **85**(14), 4971–4975 (1988).
3. D. A. Boas, M. A. Franceschini, A. K. Dunn, G. Strangman, "Noninvasive imaging of cerebral activation with diffuse optical tomography," Chapter 8 in: *In Vivo Optical Imaging of Brain Function*, R. D. Frostig (ed.), CRC Press (2002).
4. B. Chance, B. Schoener, R. Oshino, F. Itshak, Y. Nakase, "Oxidation-reduction ratio studies of mitochondria in freeze-trapped samples. NADH and flavoprotein fluorescence signals," *J. Biol. Chem.* **254**(11), 4764–4771 (1979).
5. M Cope, The development of a near infrared spectroscopy system and its application for noninvasive monitoring of cerebral blood and tissue oxygenation in the new born infant, University College London (1991).

6. F. F. Jobsis, "Noninvasive infrared monitoring of cerebral and myocardial oxygen sufficiency and circulatory parameters," *Science* **198**(4323), 1264−1267 (1977).
7. J. P. Culver, T. Durduran, D. Furuya, C. Cheung, J. H. Greenberg, A. G. Yodh, "Diffuse optical tomography of cerebral blood flow, oxygenation, and metabolism in rat during focal ischemia," *J. Cereb. Blood Flow Metab.* **23**(8), 911−924 (2003).
8. E. M. Sevick, B. Chance, J. Leigh, S. Nioka, M. Maris, "Quantitation of time- and frequency-resolved optical spectra for the determination of tissue oxygenation," *Anal. Biochem.* **195**(2), 330−351 (1991).
9. G. A. Millikan, "Experiments on muscle haemoglobin *in vivo*: The instantaneous measurement of muscle metabolism," *Proc. R. Soc. Lond. B* **123**, 218−241 (1937).
10. B. Chance, Q. Luo, S. Nioka, D. C. Alsop, J. A. Detre, "Optical investigations of physiology. A study of intrinsic and extrinsic biomedical contrast," *Philos. Trans. R. Soc. Lond. B. Biol. Sci.* **352**(1354), 707−716 (1997).
11. B. Chance, M. T. Dait, C. Zhang, T. Hamaoka, F. Hagerman, "Recovery from exercise-induced desaturation in the quadriceps muscles of elite competitive rowers," *Am. J. Physiol.* **262**, C766−C775 (1992).
12. B. Chance, C. Hirth, C. Hyman, Q. Luo, S. Nioka, "fNIRI functional imaging with near infrared," *Brain 97: 18th International Symposium on Cerebral Blood Flow and Metabolism*, Baltimore, 1997.
13. S. P. Gopinath, C. S. Robertson, C. F. Contant, R. K. Narayan, R. G. Grossman, B. Chance, "Early detection of delayed traumatic intracranial hematomas using near infrared spectroscopy," *J. Neurosurgery* **83**, 438−444 (1995).
14. D. M. Hueber, M. A. Franceschini, H. Y. Ma, Q. Zhang, J. R. Ballesteros, S. Fantini, D. Wallace, V. Ntziachristos, B. Chance, "Non-invasive and quantitative near-infrared haemoglobin spectrometry in the piglet brain during hypoxic stress, using a frequency-domain multidistance instrument," *Phys. Med. Biol.* **46**(1), 41−62 (2001).
15. B. Khan, F. Tian, K. Behbehani, M. I. Romero, M. R. Delgado, N. J. Clegg, L. Smith, D. Reid, H. Liu, G. Alexandrakis, "Identification of abnormal motor cortex activation patterns in children with cerebral palsy by functional near-infrared spectroscopy," *J. Biomed. Opt.* **15**(3), 036008 (2010).
16. S. Nioka, Q. Luo, B. Chance, "Human brain functional imaging with reflectance CWS," *Adv. Exp. Med. Biol.* **428**, 237−242 (1997).
17. B. Chance, S. Nioka, S. Sadi, C. Li, "Oxygenation and blood concentration changes in human subject prefrontal activation by anagram solutions," *Adv. Exp. Med. Biol.* **510**, 397−401 (2003).
18. C. Du, A. P. Koretsky, I. Izrailtyan, H. Benveniste, "Simultaneous detection of blood volume, oxygenation, and intracellular calcium changes during cerebral ischemia and reperfusion *in vivo* using diffuse reflectance and fluorescence," *J. Cereb. Blood Flow Metab.* **25**(8), 1078−1092 (2005).
19. E. D. London, K. R. Bonson, M. Ernst, S. Grant, "Brain imaging studies of cocaine abuse: Implications for medication development," *Crit. Rev. Neurobiol.* **13**(3), 227−242 (1999).
20. T. A. Fralix, F. W. Heineman, R. S. Balaban, "Effects of tissue absorbance on NAD(P)H and Indo-1 fluorescence from perfused rabbit hearts," *FEBS.* **262**(2), 287−292 (1990).
21. R. Brandes, V. M. Figueredo, S. A. Camacho, B. M. Massie, M. W. Weiner, "Suppression of motion artifacts in fluorescence spectroscopy of perfused hearts," *Am. J. Physiol.* **263**, H972−H980 (1992).
22. A. P. Koretsky, L. A. Katz, R. S. Balaban, "Determination of pyridine nucleotide fluorescence from the perfused heart using an internal standard," *Am. J. Physiol.* **253**, H856−H862 (1987).
23. C. Du, G. A. MacGowan, D. L. Farkas, A. P. Koretsky, "Calcium measurements in perfused mouse heart: Quantitating fluorescence and absorbance of Rhod-2 by application of photon migration theory," *J. Biophys.* **80**(1), 549−561 (2001).
24. A. K. Dunn, A. Devor, H. Bolay, M. L. Andermann, M. A. Moskowitz, A. M. Dale, D. A. Boas, "Simultaneous imaging of total cerebral hemoglobin concentration, oxygenation, and blood flow during functional activation," *Opt. Lett.* **28**(1), 28−30 (2003).
25. H. F. Zhang, K. Maslov, L. H. Wang, "Imaging of hemoglobin oxygen saturation variations in single vessels *in vivo* using photoacoustic microscopy," *Appl. Phys. Lett.* **90**(5), 053901 (2007).
26. Z. Luo, Z. Yuan, Y. Pan, C. Du, "Simultaneous imaging of cortical hemodynamics and blood oxygenation change during cerebral ischemia using dual-wavelength laser speckle contrast imaging," *Opt. Lett.* **34**(9), 1480−1482 (2009).
27. Z. Yuan, Z. Luo, N. D. Volkow, Y. Pan, C. Du, "Imaging separation of neuronal from vascular effects of cocaine on rat cortical brain *in vivo*," *Neuroimage* **54**(2), 1130−1139 (2011).